

Approximate amplitude encoding in shallow parameterized quantum circuits and its application to financial market indicator

Kouhei Nakaji,^{1,2} Shumpei Uno,^{3,2} Yohichi Suzuki,² Rudy Raymond,^{4,2} Tamiya Onodera,^{4,2}
Tomoki Tanaka,^{5,2,1} Hiroyuki Tezuka,^{6,2,1} Naoki Mitsuda,^{7,2} and Naoki Yamamoto^{2,8}

¹Graduate School of Science and Technology, Keio University,
3-14-1 Hiyoshi, Kohoku-ku, Yokohama, Kanagawa, 223-8522, Japan

²Quantum Computing Center, Keio University, 3-14-1 Hiyoshi,
Kohoku-ku, Yokohama, Kanagawa, 223-8522, Japan

³Mizuho Information & Research Institute, Inc.,
2-3 Kanda-Nishikicho, Chiyoda-ku, Tokyo, 101-8443, Japan

⁴IBM Quantum, IBM Research-Tokyo, 19-21 Nihonbashi Hakozaki-cho, Chuo-ku, Tokyo, 103-8510, Japan

⁵Mitsubishi UFJ Financial Group, Inc. and MUFG Bank, Ltd.,
2-7-1 Marunouchi, Chiyoda-ku, Tokyo, 100-8388, Japan

⁶Sony Corporation, 1-7-1 Konan, Minato-ku, Tokyo, 108-0075, Japan

⁷Sumitomo Mitsui Trust Bank, Ltd., 1-4-1, Marunouchi, Chiyoda-ku, Tokyo, 100-8233, Japan

⁸Department of Applied Physics and Physico-Informatics,
Keio University, Hiyoshi 3-14-1, Kohoku-ku, Yokohama 223-8522, Japan

Efficient methods for loading given classical data into quantum circuits are essential for various quantum algorithms. In this paper, we propose an algorithm called *Approximate Amplitude Encoding* that can effectively load all the components of a given real-valued data vector into the amplitude of quantum state, while the previous proposal can only load the absolute values of those components. The key of our algorithm is to variationally train a shallow parameterized quantum circuit, using the results of two types of measurement; the standard computational-basis measurement plus the measurement in the Hadamard-transformed basis, introduced in order to handle the sign of the data components. The variational algorithm changes the circuit parameters so as to minimize the sum of two costs corresponding to those two measurement basis, both of which are given by the efficiently-computable maximum mean discrepancy. We also consider the problem of constructing the singular value decomposition entropy via the stock market dataset to give a financial market indicator; a quantum algorithm (the variational singular value decomposition algorithm) is known to produce a solution faster than classical, which yet requires the sign-dependent amplitude encoding. We demonstrate, with an in-depth numerical analysis, that our algorithm realizes loading of time-series of real stock prices on quantum state with small approximation error, and thereby it enables constructing an indicator of the financial market based on the stock prices.

I. INTRODUCTION

Quantum computing is expected to solve problems that cannot be solved efficiently by any classical means. Particular promising quantum algorithms are of course Shor's factoring algorithm [1] and Grover search algorithm [2]. Later the Harrow-Hassidim-Lloyd (HHL) algorithm [3] was proposed, which offers exponential speedup for solving general linear algebraic equations, and opened the door of applicability of quantum computing in machine learning, as it enhances various linear algebraic sub-routines [4–10].

An important caveat on HHL is that it assumes that the classical data (i.e., elements of the linear equation) has been loaded into the (real) amplitude of a quantum state. Beyond HHL, moreover, some quantum algorithms assume such *amplitude encoding* [11–15]. However, exponential number of quantum gates are in general required for realizing the amplitude encoding [16–19], which might destroy the quantum advantage. Therefore, a method for efficient amplitude encoding realizable with polynomial numbers of gate operations is highly demanded, but it has been a missing piece.

In this paper, we propose an algorithm called the *ap-*

proximate amplitude encoding (AAE) that trains a shallow parameterized quantum circuit (PQC) to approximate the ideal data receiver. To describe more precisely, let $|Data\rangle$ be the target n -qubit state whose amplitude represents the classical data component. Then our algorithm provides the training policy of a PQC represented by the unitary $U(\theta)$, so that the finally obtained $U(\theta)$ followed by another shallow circuit V approximately generates $|Data\rangle$, with the help of an auxiliary qubit. Namely, as a result of training, $VU(\theta)|0\rangle^{\otimes n}|0\rangle$ approximates the state $e^{i\alpha}|Data\rangle|y\rangle$, where $|y\rangle$ is a state of the auxiliary qubit and $e^{i\alpha}$ is the global phase.

Hence, though there appears an approximation error, the $O(1) \sim O(poly(n))$ -depth quantum circuit $VU(\theta)$ achieves the data loading, instead of the ideal exponential-depth circuit. It should also be mentioned that the spatial complexity for storing the data in a classical memory is $O(2^n)$, while that in quantum is $O(poly(n))$ (\propto the number of parameters), which is also beneficial.

Our work is motivated by Ref. [20] that proposed a variational algorithm for constructing an approximate quantum data-receiver, in the framework of generative adversarial network (GAN); the idea is to train a shal-

low PQC so that the absolute values of the amplitude of the final state approximate the absolute values of the data vector components. Hence the method is limited to the case where the sign of the data components does not matter or the case where the data is given by a probability vector as in the setting of [20]. In other words, this method cannot be applied to a quantum algorithm based on the amplitude encoding, e.g., HHL [3], which needs loading the classical data without dropping their sign. In contrast, our proposed method can correctly encode the sign in addition to the absolute value, hence in principle it is applicable to all such amplitude-encoding-based algorithms.

As another contribution of this paper, we show that the combination of our AAE algorithm and the variational *quantum Singular Value Decomposition (qSVD)* algorithm [21] offers a new efficient and scalable quantum algorithm for computing the *SVD entropy* for stock price dynamics [22], which is used as a good indicator of the financial market. In fact, this algorithm requires that the signs of the stock price data is correctly loaded into the quantum amplitudes. We give an in-depth numerical simulation with a set of real stock price data, to demonstrate that this algorithm generates a good approximating solution of the correct SVD entropy.

The rest of the paper is organized as follows. In Section II, we state our proposed algorithm. Section III gives a demonstration of the approximate amplitude encoding by computing the SVD entropy for stock market dynamics. Finally, we conclude with some remarks in Section IV.

II. ALGORITHM

A. The goal of Approximate Amplitude Encoding

In quantum algorithms that process a classical data represented by a real-valued N -dimensional vector \mathbf{d} , first it has to be encoded into the quantum state; a particular encoding that can potentially be linked to quantum advantage is to encode \mathbf{d} to the amplitude of an n -qubits state $|Data\rangle$. More specifically, given $|j\rangle$ as $|j\rangle = |j_1 j_2 \cdots j_n\rangle$ where j_k is the state of the k -th qubit in computational basis and $j = \sum_{k=1}^n 2^{n-k} j_k$, the data quantum state is given by

$$|Data\rangle = \sum_{j=0}^{N-1} \mathbf{d}_j |j\rangle, \quad (1)$$

where $N = 2^n$ and \mathbf{d}_j denotes the j -th element of the vector \mathbf{d} . Also here \mathbf{d} is normalized; $\sum_j \mathbf{d}_j^2 = 1$. Recall that, even when all the elements of \mathbf{d} are fully accessible, in general, a quantum circuit for generating the state (1) requires an exponential number of gates, which might destroy the quantum advantage.

In contrast, our algorithm uses a ℓ -depth PQC (hence composed of $O(\ell n)$ gates) to try to approximate the ideal

state (1). The depth ℓ is set to be $O(1) \sim O(poly(n))$. Suppose now that, given an N -dimensional vector \mathbf{a} , the state generated by a PQC, represented by the unitary matrix $U(\theta)$ with θ the vector of parameters, is given by $U(\theta)|0\rangle^{\otimes n} = \sum_{j=0}^{N-1} \mathbf{a}_j |j\rangle$. If the probability to have $|j\rangle$ as a result of measurement in the computational basis is \mathbf{d}_j^2 , this means $|\mathbf{a}_j| = |\mathbf{d}_j|$ for all j . Therefore, if only the absolute values of the amplitudes are necessary in a quantum algorithm after the data loading as in the case of [20], the goal is to train $U(\theta)$ so that the following condition is satisfied;

$$|\mathbf{a}_j|^2 = |\langle j|U(\theta)|0\rangle|^2 \simeq \mathbf{d}_j^2, \quad \forall j \in [0, 1, \dots, N-1]. \quad (2)$$

However, some quantum algorithms such as HHL [3] need a quantum state containing \mathbf{d}_j itself, rather than \mathbf{d}_j^2 . Naively, hence, the goal is to train $U(\theta)$ so that $U(\theta)|0\rangle^{\otimes n} \simeq |Data\rangle$. But as will be discussed later, in general we need an auxiliary qubit and thereby aim to train $U(\theta)$ so that

$$VU(\theta)|0\rangle^{\otimes n}|0\rangle \simeq e^{i\alpha}|Data\rangle|y\rangle, \quad (3)$$

where V represents a fixed operator containing post-selection and $e^{i\alpha}$ is the global phase. $|0\rangle$ in the left hand side and $|y\rangle$ in the right hand are the auxiliary qubit state, which might not be necessary in a particular case (Case 1 shown later). This is the goal of the proposed AAE algorithm. When Eq. (3) is satisfied, the first n -qubits of $VU(\theta)|0\rangle^{\otimes n}$ serve as an input of the subsequent quantum algorithm.

B. The proposed algorithm

This section is twofold; first we identify a condition that guarantees the equality in Eq. (3); then, based on this condition, we specify a valid cost function and describe the design procedure of $U(\theta)$. The algorithm depends on the following two cases related to the elements of target \mathbf{d} :

(Case 1) The elements of \mathbf{d} are all non-positive or all non-negative.

(Case 2) Otherwise.

Condition for the perfect encoding

In Case 1, we consider the following two conditions:

$$|\langle j|U(\theta)|0\rangle^{\otimes n}|^2 = \mathbf{d}_j^2 \quad (4)$$

$$\begin{aligned} |\langle j|H^{\otimes n}U(\theta)|0\rangle^{\otimes n}|^2 &= \left(\sum_{k=0}^{N-1} \mathbf{d}_k \langle j|H^{\otimes n}|k\rangle \right)^2 \\ &\equiv (\mathbf{d}_j^H)^2 \end{aligned} \quad (5)$$

Note that \mathbf{d}_j^H is classically computable with complexity $O(N \log N)$, by using the Walsh-Hadamard transform [23]. The above condition guarantees that our goal is exactly satisfied, as stated in the following theorem (the proof is found in Appendix A):

Theorem 1. *In Case 1, if the n -qubits PQC $U(\theta)$ satisfies Eqs. (4) and (5), then $U(\theta)|0\rangle^{\otimes n} = \sum_j \mathbf{d}_j|j\rangle$ or $U(\theta)|0\rangle^{\otimes n} = -\sum_j \mathbf{d}_j|j\rangle$ holds.*

Hence, this theorem implies that, if (4) and (5) are “almost” satisfied, then we may have $U(\theta)|0\rangle^{\otimes n} \simeq \pm|Data\rangle$, which is our goal (3).

In Case 2, i.e., the case where some (not all) elements of \mathbf{d} are non-negative while the others are positive, the target state $|Data\rangle$ can be decomposed to

$$|Data\rangle = |Data^+\rangle + |Data^-\rangle, \quad (6)$$

where the amplitudes of $|Data^+\rangle$ are positive and those of $|Data^-\rangle$ are non-positive. Then, by introducing an auxiliary single qubit, we can represent the state $|Data\rangle$ in the form considered in Case 1; that is, the amplitudes of the $(n+1)$ -qubits state

$$|\bar{\psi}\rangle \equiv |Data^+\rangle|0\rangle - |Data^-\rangle|1\rangle \quad (7)$$

are non-negative and $\langle\bar{\psi}|\bar{\psi}\rangle = 1$. We write this state as $|\bar{\psi}\rangle = \sum_{i=0}^{2N-1} \bar{\mathbf{d}}_i|j\rangle$ in terms of the computational basis $\{|j\rangle\}$ and the corresponding $2N$ -dimensional vector $\bar{\mathbf{d}}$. Then, Theorem 1 states that, if the condition

$$|\langle j|U(\theta)|0\rangle^{\otimes n+1}|^2 = \bar{\mathbf{d}}_j^2 \quad (8)$$

$$|\langle j|H^{\otimes n+1}U(\theta)|0\rangle^{\otimes n+1}|^2 = \left(\sum_{k=0}^{2N-1} \bar{\mathbf{d}}_k \langle j|H^{\otimes n+1}|k\rangle \right)^2 \quad (9)$$

$$\equiv (\bar{\mathbf{d}}_j^H)^2$$

are satisfied, then $U(\theta)|0\rangle^{\otimes n+1} = \pm|\bar{\psi}\rangle$ holds. Further, once we obtain $|\bar{\psi}\rangle$, this gives us the target $|Data\rangle$, via the following procedure. That is, operating the Hadamard transform to the last auxiliary qubit yields

$$I^{\otimes n} \otimes H|\bar{\psi}\rangle = \frac{|Data^+\rangle - |Data^-\rangle}{\sqrt{2}}|0\rangle + \frac{|Data^+\rangle + |Data^-\rangle}{\sqrt{2}}|1\rangle, \quad (10)$$

and then the post-selection of $|1\rangle$ via the measurement on the last qubit in Eq. (10) gives us $|Data\rangle$ in the first n -qubits. The above result is summarized as follows.

Theorem 2. *In Case 2, suppose that the $(n+1)$ -qubits PQC $U(\theta)$ satisfies Eqs. (8) and (9). Then, if the measurement result of the last qubit in the computational basis for the state $(I^{\otimes n} \otimes H)U(\theta)|0\rangle^{\otimes n+1}$ is $|1\rangle$, then $|Data\rangle$ is generated. That is,*

$$(I^{\otimes n} \otimes |1\rangle\langle 1|)(I^{\otimes n} \otimes H)U(\theta)|0\rangle^{\otimes n+1} \propto |Data\rangle|1\rangle.$$

This theorem implies that, if $U(\theta)$ is trained so that the conditions (8) and (9) are “almost” satisfied, a state close to $|Data\rangle$ can be obtained by the above post-selection procedure, with success probability nearly 1/2. The overview of the data-loading algorithm, except the details of the training policy of $U(\theta)$, is summarized in Fig. 1.

Optimization of $U(\theta)$

Here we provide a training method for optimizing $U(\theta)$, so that Eqs. (4) and (5) are nearly satisfied in Case 1, and Eqs. (8) and (9) are nearly satisfied in Case 2, with as small approximation error as possible. For this purpose, we employ the strategy to decrease the *maximum mean discrepancy (MMD)* cost, which was previously proposed for training Quantum Born Machine [24, 25]. Note that the other costs, the Stein discrepancy [25] and the Sinkhorn divergence [25] can also be taken, but in this paper we use MMD for its ease of use.

The MMD is a cost of the discrepancy between two probability distributions: $q_\theta(j)$, the model probability distribution, and $p(j)$, the target distribution. The cost function $\mathcal{L}_{MMD}(q_\theta, p)$ is defined as

$$\mathcal{L}_{MMD}(q_\theta, p) \equiv \gamma_{MMD}(q_\theta, p)^2, \quad \gamma_{MMD}(q_\theta, p) = \left| \sum_{j=0}^{N-1} q_\theta(j)\Phi(j) - \sum_{j=0}^{N-1} p(j)\Phi(j) \right|, \quad (11)$$

where $\Phi(j)$ is a function that maps j to a feature space. Thus, given the kernel $\kappa(j, k)$ as $\kappa(j, k) = \Phi(j)^T \Phi(k)$, it holds

$$\mathcal{L}_{MMD}(q_\theta, p) = \mathbf{E}_{\substack{j \sim q_\theta \\ k \sim q_\theta}} [\kappa(j, k)] - 2 \mathbf{E}_{\substack{j \sim q_\theta \\ k \sim p}} [\kappa(j, k)] + \mathbf{E}_{\substack{j \sim p \\ k \sim p}} [\kappa(j, k)]. \quad (12)$$

Note that when the kernel is *characteristic* [26, 27], then $\mathcal{L}_{MMD}(q_\theta, p) = 0$ means $q_\theta(j) = p(j)$ for all j . In this paper, we take the Gaussian kernel, which is characteristic.

In Case 1, the goal is to train the model distributions

$$q_\theta(j) = |\langle j|U(\theta)|0\rangle^{\otimes n}|^2, \quad q_\theta^H(j) = |\langle j|H^{\otimes n+1}U(\theta)|0\rangle^{\otimes n}|^2$$

so that they approximate the target distributions

$$p(j) = \mathbf{d}_j^2, \quad p^H(j) = (\mathbf{d}_j^H)^2, \quad (13)$$

respectively. In Case 2, the model distributions

$$q_\theta(j) = |\langle j|U(\theta)|0\rangle^{\otimes n+1}|^2, \quad q_\theta^H(j) = |\langle j|H^{\otimes n+1}U(\theta)|0\rangle^{\otimes n+1}|^2$$

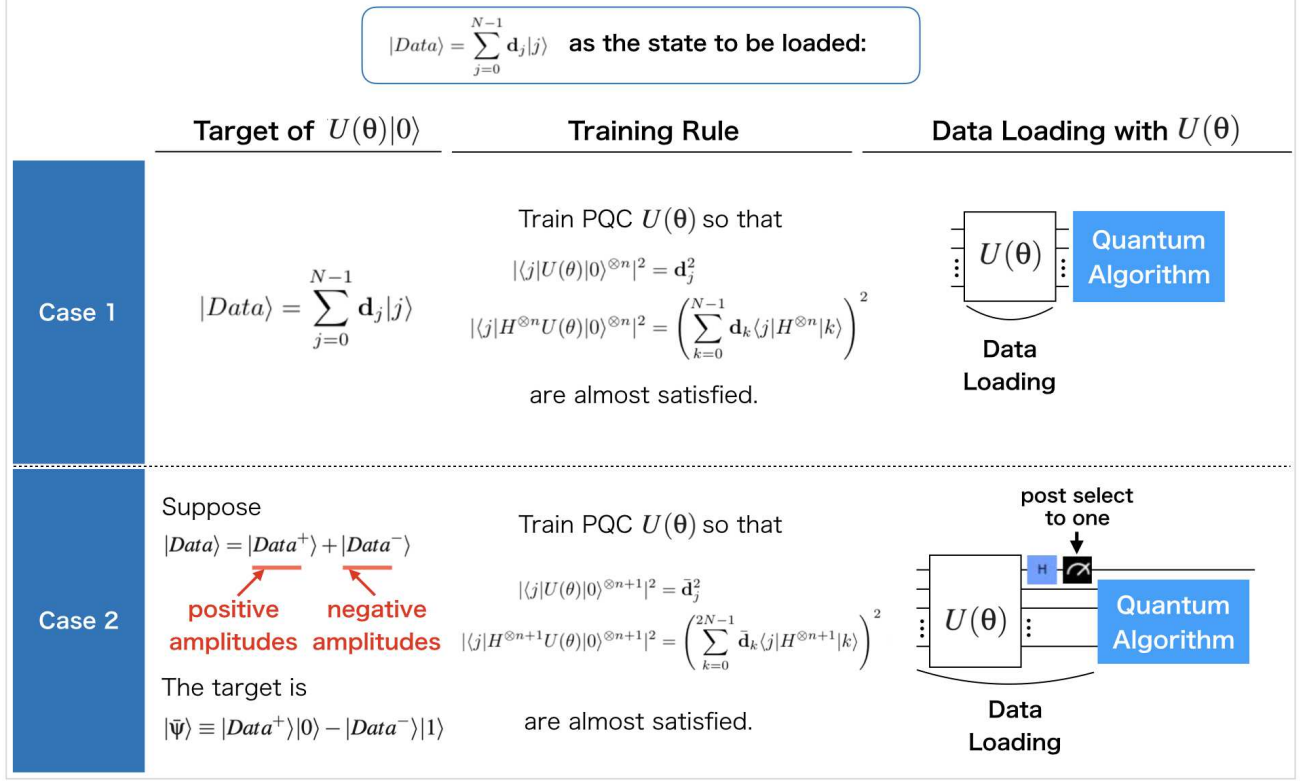


FIG. 1: Overview of the Approximate Amplitude Encoding algorithm in Case 1 and Case 2.

are trained so that they approximate the target distributions

$$p(j) = \bar{\mathbf{d}}_j^2, \quad p^H(j) = \bar{\mathbf{d}}_j^{H2}, \quad (14)$$

respectively. In both cases, our training policy is to minimize the following cost function:

$$\mathcal{L}(\theta) = \frac{\mathcal{L}_{MMD}(q_\theta, p) + \mathcal{L}_{MMD}(q_\theta^H, p^H)}{2}. \quad (15)$$

Actually, $\mathcal{L}(\theta)$ becomes zero if and only if $\mathcal{L}_{MMD}(q_\theta, p) = 0$ and $\mathcal{L}_{MMD}(q_\theta^H, p^H) = 0$, or equivalently $q_\theta(j) = p(j)$ and $q_\theta^H(j) = p^H(j)$ for all j as long as we use a characteristic kernel.

To minimize the cost function (15), we take the standard gradient descent algorithm. In particular we consider the PQC where each parameter θ_r is embedded in the quantum circuit in the form $\exp(-i\theta_r P_r)$ with P_r a single qubit Hermitian operator satisfying $P_r^2 = \mathbf{1}$ (typically the Pauli matrix). In this case, the gradient of \mathcal{L}

with respect to θ_r can be explicitly computed as

$$\begin{aligned} 2 \frac{\partial \mathcal{L}}{\partial \theta_r} = & \mathbf{E}_{\substack{j \sim q_{\theta_r}^+ \\ k \sim q_\theta}} [\kappa(j, k)] - \mathbf{E}_{\substack{j \sim q_{\theta_r}^- \\ k \sim q_\theta}} [\kappa(j, k)] \\ & - \mathbf{E}_{\substack{j \sim q_{\theta_r}^+ \\ k \sim p}} [\kappa(j, k)] + \mathbf{E}_{\substack{j \sim q_{\theta_r}^- \\ k \sim p}} [\kappa(j, k)] \\ & + \mathbf{E}_{\substack{j \sim q_{\theta_r}^{H+} \\ k \sim q_\theta^H}} [\kappa(j, k)] - \mathbf{E}_{\substack{j \sim q_{\theta_r}^{H-} \\ k \sim q_\theta^H}} [\kappa(j, k)] \\ & - \mathbf{E}_{\substack{j \sim q_{\theta_r}^{H+} \\ k \sim p^H}} [\kappa(j, k)] + \mathbf{E}_{\substack{j \sim q_{\theta_r}^{H-} \\ k \sim p^H}} [\kappa(j, k)], \end{aligned} \quad (16)$$

where $q_{\theta_r}^\pm(j) = |\langle j|U_{r\pm}(\theta)|0\rangle|^2$, $q_{\theta_r}^{H\pm}(j) = |\langle j|HU_{r\pm}(\theta)|0\rangle|^2$, and

$$\begin{aligned} U_{r\pm}(\theta) &= U_{r\pm}(\{\theta_1, \dots, \theta_{r-1}, \theta_r, \theta_{r+1}, \dots, \theta_R\}) \\ &= U(\{\theta_1, \dots, \theta_{r-1}, \theta_r \pm \pi/2, \theta_{r+1}, \dots, \theta_R\}), \end{aligned} \quad (17)$$

with R as the number of the parameters [24]. Therefore, the gradient (16) can be approximately computed by sampling j and k from the distributions q_θ , $q_{\theta_r}^+$, $q_{\theta_r}^-$, q_θ^H , $q_{\theta_r}^{H+}$, $q_{\theta_r}^{H-}$, p , and p^H . Then using the gradient descent algorithm with Eq. (16), we can update the values of $\theta = (\theta_1, \dots, \theta_R)$ to the direction that minimizes $\mathcal{L}(\theta)$.

Note that exponential number of measurements is not necessary for the optimization, if the goal is to find θ satisfying $\mathcal{L}(\theta) < \epsilon$ with ϵ a fixed approximation error; we can choose ϵ , depending on how precisely the data needs to be loaded. Namely, the total number of measurements $N_{\text{total}}(\epsilon)$, required to satisfy $\mathcal{L}(\theta) < \epsilon$ with high probability, does not depend on N but depends on the number of measurements in each iteration step N_{shot} and ϵ . One reason why $N_{\text{total}}(\epsilon)$ does not depend on N is that the estimation error of the gradient (16) does not depend on N but depends on N_{shot} . In [28] (see also [25]), it is shown that the estimation error of $\gamma_{\text{MMD}}(q_\theta, p)$ defined in (11) is bounded by $O(1/\sqrt{N_{\text{shot}}})$ when N_{shot} samples are obtained from q_θ and p for computing $\gamma_{\text{MMD}}(q_\theta, p)$, and therefore, the estimation error of $\mathcal{L}_{\text{MMD}}(q_\theta, p)$ is also bounded by $O(1/\sqrt{N_{\text{shot}}})$. Similarly, it can be shown that the estimation error of the cost function (15) and that of its gradients are also bounded by $O(1/\sqrt{N_{\text{shot}}})$. Another reason is that the space where the optimization is performed is a relatively low-dimensional parameter space. For instance, when \mathcal{L} is convex, the total number of iterations for realizing $\mathcal{L}(\theta) < \epsilon$ is $O(GS/\epsilon^2)$ when using the stochastic gradient descent with an appropriate step size [29], where G is the upper bound of $|\partial\mathcal{L}/\partial\theta_r|$ over the parameter space, and S is a constant that relates with the size of the parameter space.

C. Some remarks

Remark 1: As shown above, in Case 2, the encoding can be carried out with success probability 1/2 in the ideal case (i.e., the case where Eqs. (8) and (9) are exactly satisfied). But by applying the amplitude amplification operation [30], we obtain $|Data\rangle$ with success probability 1, instead of 1/2, although more gates to implement this extra operation are required. The method is described as follows, in the ideal case. It holds

$$\begin{aligned} & \pm U(\theta) \otimes H \otimes H |0\rangle^{\otimes n} |0\rangle |0\rangle \\ &= \frac{|Data^+\rangle - |Data^-\rangle}{2} |00\rangle + \frac{|Data^+\rangle - |Data^-\rangle}{2} |01\rangle \\ &+ \frac{|Data^+\rangle + |Data^-\rangle}{2} |10\rangle + \frac{|Data^+\rangle + |Data^-\rangle}{2} |11\rangle \end{aligned} \quad (18)$$

Similar to [31, 32], the amplitude amplification operator \mathcal{Q} can be defined as

$$\mathcal{Q} \equiv \mathcal{A}(I_{n+2} - 2|0\rangle_{n+2}\langle 0|_{n+2})\mathcal{A}^\dagger(I_{n+2} - 2I_n \otimes |11\rangle\langle 11|),$$

where $\mathcal{A} \equiv U(\theta) \otimes H \otimes H$. Then by applying \mathcal{Q} to the state (18), we have

$$\mathcal{Q}\mathcal{A}|0\rangle^{\otimes n} |0\rangle |0\rangle = \pm |Data\rangle |1\rangle |1\rangle.$$

Thus, $|Data\rangle$ is obtained with probability 1 (by ignoring the last two qubits).

Remark 2: As mentioned in Section I, the motivating work [20] used GAN [33] to train the PQC to learn a probability distribution of the absolute values of data. In our work, in contrast, we do not take the GAN formulation. The main reason is that, in our case, the PQC is trained to learn *two* probability distributions (Eqs. (4) and (5) in Case 1), which cannot be formulated in the ordinary GAN that handles only one generator and one discriminator. Customizing GAN to fit into our setting may be doable, but the training policy may become more involved.

Remark 3: Readers may wonder if the Kullback–Leibler divergence (KL-divergence)

$$\mathcal{L}_{\text{KL}}(p, q_\theta) = \sum_j \left[p(j) \log(p(j)) - p(j) \log(q_\theta(j)) \right] \quad (19)$$

would be a more natural cost function than MMD for comparing a target distribution $p(j)$ and a model distribution $q_\theta(j)$ with parameter θ . The gradient $\partial\mathcal{L}_{\text{KL}}/\partial\theta_r$ is given by

$$\frac{\partial\mathcal{L}_{\text{KL}}}{\partial\theta_r} = - \sum_j \frac{p(j)}{q_\theta(j)} \frac{\partial q_\theta(j)}{\partial\theta_r}, \quad (20)$$

which thus requires the computation of $q_\theta(j)$. Now in the quantum case, typically, we take $q_\theta(j) = |\langle j|U(\theta)|0\rangle^{\otimes n}|^2$. However, in general, this quantity needs an exponential number of measurements to precisely compute. Therefore, the gradient of the KL-divergence cannot be efficiently computed in the quantum case, unlike the case of MMD.

Remark 4: In Case 1, we train $U(\theta)$ so that (4) and (5) are approximately satisfied; the complexity for computing the right hand side of (5) is $O(N\log N)$. However, as we see the proof of Theorem 1, even if the condition (5) changes to

$$|\langle 0|H^{\otimes n}U(\theta)|0\rangle^{\otimes n}|^2 = \left(\sum_{k=0}^{N-1} \mathbf{d}_k \langle 0|H^{\otimes n}|k\rangle \right)^2, \quad (21)$$

we can show $U(\theta)|0\rangle = \sum_j \mathbf{d}_j |j\rangle$ or $U(\theta)|0\rangle = -\sum_j \mathbf{d}_j |j\rangle$. This implies that we can obtain the data loading circuit by training $U(\theta)$ so that (4) and (21) are approximately satisfied. Then the complexity for computing the right hand side is reduced to $O(N)$. In Case 2, the situation is the same. Therefore, building an algorithm by using the conditions (4) and (21) can be a good direction for future work.

Remark 5: Readers may wonder that, if we carefully choose an operator X instead of $H^{\otimes n}$, the following conditions:

$$|\langle j|U(\theta)|0\rangle^{\otimes n}|^2 = \mathbf{d}_j^2 \quad (22)$$

$$|\langle j|XU(\theta)|0\rangle^{\otimes n}|^2 = \left(\sum_{k=0}^{N-1} \mathbf{d}_k \langle j|X|k\rangle \right)^2 \quad (23)$$

result in $U(\theta)|0\rangle = \sum_j \mathbf{d}_j|j\rangle$ or $U(\theta)|0\rangle = -\sum_j \mathbf{d}_j|j\rangle$ for arbitrary real vector \mathbf{d} . If so, it is favorable because we do not need Case 2; namely, we do not need neither auxiliary qubits nor the post-selection. However, as shown in the discussion in Appendix B, it seems to be difficult to find such X for arbitrary \mathbf{d} . That is why we prepare the two cases depending on \mathbf{d} and build the algorithm for each case.

III. APPLICATION TO SVD ENTROPY CALCULATION FOR FINANCIAL MARKET INDICATOR

This section is devoted to describe the quantum algorithm composed of our AAE and the variational qSVD algorithm [21] for computing the SVD entropy for stock price dynamics [22]. We first give the definition of SVD entropy and then describe the quantum algorithm, with particular emphasis on how the AAE algorithm well fits into the problem of computing the SVD entropy. Finally the in-depth numerical simulation is provided.

A. SVD Entropy

The SVD entropy is used as one of the good indicators for forewarning the financial crisis, which is computed by the singular value decomposition of the correlation matrix between stock prices. Let $s_{j,t}$ be the price of the j th stock at time t . Then we define the logarithmic rate of return as follows;

$$r_{jt} = \log(s_{j,t}) - \log(s_{j,t-1}). \quad (24)$$

Also, the correlation matrix C of the set of stocks $j = 1, 2, \dots, N_s$ over the term $t = 1, 2, \dots, T$ is defined as

$$C_{jk} = \sum_{t=1}^T a_{jt} a_{kt}, \quad (25)$$

where

$$a_{jt} = \frac{r_{jt} - \langle r_j \rangle}{\sigma_j \sqrt{N_s T}}. \quad (26)$$

The average $\langle r_j \rangle$ and the standard deviation σ_j over the whole period of term are defined as

$$\langle r_j \rangle = \frac{1}{T} \sum_{t=1}^T r_{jt}, \quad \sigma_j^2 = \frac{1}{T} \sum_{t=1}^T (r_{jt} - \langle r_j \rangle)^2. \quad (27)$$

The correlation matrix C is positive semi-definite, and thus its eigenvalues are non-negative. In addition, C satisfies

$$\text{Tr}(C) = \sum_{j=1}^{N_s} \sum_{t=1}^T a_{jt}^2 = 1. \quad (28)$$

Now for the positive eigenvalues $\lambda_1, \lambda_2, \dots, \lambda_U$ of the correlation matrix, which satisfy $\sum_{u=1}^U \lambda_u = 1$ from Eq. (28), the SVD entropy S is defined as

$$S = - \sum_{u=1}^U \lambda_u \log \lambda_u. \quad (29)$$

Computation of S in any classical means requires the diagonalization of the $N_s \times N_s$ matrix C , hence its computational complexity is $O(N_s^3)$.

As usual, S quantifies the randomness of the probability distribution $\{\lambda_u\}$, but it offers an additional information regarding the financial status in terms of stock market. It is known that a few eigenvalues of C are much larger than what is predicted by the random matrix theory [34–37], implying that the corresponding eigenvectors may have meaningful interpretation in the financial sense, as follows. That is, the eigenvector associated with the largest eigenvalue is interpreted as the market portfolio, which consists of the entire stocks, and the eigenvectors associated with the other large eigenvalues are interpreted as the portfolios of stocks belonging to different industrial sectors. The structural relation of these eigenvectors does not change a lot during the normal periods, but it changes drastically at a point related to financial crisis. Actually, during such an abnormal period, the stock prices across the entire market or the clusters of several industrial sectors show similar behavior; mathematically, this means that the eigenvalues become nearly degenerate, or roughly speaking the probability distribution $\{\lambda_u\}$ visibly becomes sharp. As a result, S takes a relatively small value, indicating the financial crisis. This behavior is analogous to that of the statistical mechanical systems near a critical point, where spins form a set of clusters due to the very large correlation length [38]. Lastly we add a remark that a similar and detailed analysis for image processing can be found in Ref. [39].

B. Computation on quantum devices

Computation of the SVD entropy on a quantum device can be performed by firstly training the PQC $U(\theta)$ by the AAE algorithm, to generate a target state in which the stock data a_{jt} is suitably embedded. Next, the PQC $U_{\text{SVD}}(\xi)$ is variationally trained so that it performs the SVD. Finally, the SVD entropy is estimated from the output state of the entire circuit $U_{\text{SVD}}(\xi)U(\theta)$. In the following, we show the detail discussions of the procedures.

The first part: data loading

The AAE serves as the first part of the entire algorithm; that is, it is used to load the normalized logarithmic rate of return of the stock price data a_{jt} given in Eq. (26) into a quantum state. The target state that

the AAE aims to approximate is the following bipartite state:

$$|Data\rangle = \sum_{j=1}^{N_s} \sum_{t=1}^T a_{jt} |j\rangle |t\rangle, \quad (30)$$

where $\{|j\rangle\}_{j=1,\dots,N_s}$ and $\{|t\rangle\}_{t=1,\dots,T}$ are the computational basis set constructing the stock index Hilbert space $\mathcal{H}_{\text{stock}}$ and the time index Hilbert space $\mathcal{H}_{\text{time}}$, respectively. The number of qubits needed to prepare this state is $n_s + n_t$, where $n_s = O(\log N_s)$ and $n_t = O(\log T)$, meaning that the quantum approach has an exponential advantage in the memory resource. Also note that the state (30) is normalized because of Eq. (28). The partial trace over $\mathcal{H}_{\text{time}}$ gives rise to

$$\rho_{\text{stock}} = \text{Tr}_{\mathcal{H}_{\text{time}}}(|Data\rangle\langle Data|) = \sum_{jk} C_{jk} |j\rangle\langle k|, \quad (31)$$

where C_{jk} is the (j, k) element of the correlation matrix given in Eq. (25); that is, $\rho_{\text{stock}} = C$ is realized on a quantum device. Hence, we need an efficient algorithm to diagonalize ρ_{stock} and eventually compute the SVD entropy S on a quantum device, and this is the reason why we use the qSVD algorithm.

The second part: Quantum singular value decomposition

We apply the qSVD algorithm [21] to achieve the above-mentioned diagonalization task. The point of this algorithm lies in the well known fact that diagonalizing $\rho_{\text{stock}} = C$ is equivalent to realizing the Schmidt decomposition of $|Data\rangle$:

$$|Data\rangle = \sum_{m=1}^M c_m |v_m\rangle |v'_m\rangle, \quad (32)$$

where $\{|v_m\rangle\}$ and $\{|v'_m\rangle\}$ are set of orthogonal states, with $M \leq \min(N_s, T)$; note that in general these are not the computational basis. Actually, in this representation, ρ_{stock} is calculated as

$$\rho_{\text{stock}} = \text{Tr}_{\mathcal{H}_{\text{time}}}(|Data\rangle\langle Data|) = \sum_{m=1}^M |c_m|^2 |v_m\rangle\langle v_m|,$$

which is exactly the diagonalization of $\rho_{\text{stock}} = C$. This equation tells us that the eigenvalue of the correlation matrix C is now found to be $\lambda_j = |c_j|^2$ for all $j = 1, \dots, M = U$, and thus we end up with the expression

$$S = - \sum_{m=1}^M |c_m|^2 \log |c_m|^2. \quad (33)$$

Note that S is the entanglement entropy between $\mathcal{H}_{\text{stock}}$ and $\mathcal{H}_{\text{time}}$; i.e., von Neumann entropy of ρ_{stock} , $S = -\text{Tr}(\rho_{\text{stock}} \log \rho_{\text{stock}})$.

The qSVD [21] is a variational algorithm for finding the Schmidt form (32). Let $|\widetilde{Data}\rangle$ be the output of the AAE circuit, which approximates the target $|Data\rangle$. We train PQC's $U_1(\xi)$ and $U_2(\xi')$ with parameters ξ and ξ' , so that, ideally, they realize

$$U_1(\xi) \otimes U_2(\xi') |\widetilde{Data}\rangle = \sum_{m=1}^M c_m |\bar{m}\rangle |\bar{m}\rangle. \quad (34)$$

Here, $\{|\bar{m}\rangle\}$ is a *subset* of the *computational basis* states, which thus satisfy $\langle \bar{m} | \bar{\ell} \rangle = \delta_{m,\ell}$. Clearly, then, the Schmidt basis is identified as $|v_m\rangle = U_1^\dagger(\xi) |\bar{m}\rangle$ and $|v'_m\rangle = U_2^\dagger(\xi') |\bar{m}\rangle$. The training policy is chosen so that $U_1(\xi) \otimes U_2(\xi') |\widetilde{Data}\rangle$ is as close to the Schmidt form in the computational basis as possible. The cost function to be minimized, proposed in [21], is the sum of Hamming distances between the stock bit sequence and the time bit sequence, obtained as the result of computational-basis measurement on $\mathcal{H}_{\text{stock}}$ and $\mathcal{H}_{\text{time}}$; actually, if we measure the right hand side of Eq. (34), the outcomes are perfectly correlated, e.g., 010 on $\mathcal{H}_{\text{stock}}$ and 010 on $\mathcal{H}_{\text{time}}$. When $n_s = n_t$, which is the case in our numerical demonstration, this cost function is represented as

$$\mathcal{L}_{\text{SVD}}(\xi, \xi') = \sum_{q=1}^{n_s} \frac{1 - \langle \sigma_z^q \sigma_z^{q+n_s} \rangle}{2}, \quad (35)$$

where the expectation $\langle \cdot \rangle$ is taken over $U_1(\xi) \otimes U_2(\xi') |\widetilde{Data}\rangle$. The operator σ_z^q is the Pauli Z operator that acts on the q -th qubit. We see that $\mathcal{L}_{\text{SVD}}(\xi, \xi') = 0$ holds, if and only if $U_1(\xi) \otimes U_2(\xi') |\widetilde{Data}\rangle$ takes the form of the right hand side of Eq. (34). Therefore, by training $U_1(\xi)$ and $U_2(\xi')$ so that $\mathcal{L}_{\text{SVD}}(\xi, \xi')$ is minimized, we obtain the state that best approximates the Schmidt decomposed state. Lastly, we gain the information on the amplitude of the output of qSVD circuit via the computational basis measurements. (i.e., the values approximating $|c_m|^2$) and then compute the SVD entropy.

C. Complexity of the algorithm

An algorithm for effectively estimating S from the state $\sum_{m=1}^M c_m |i_m\rangle |t_m\rangle$, has been proposed in [40]. The algorithm, which utilizes the amplitude estimation [30], can estimate S with the complexity $\tilde{O}\left(\sqrt{\min(N_s, T)}/\epsilon^2\right)$ where ϵ is the estimation error and the \tilde{O} hides the polylog factor. The computational complexity of estimating S is negligible if the quantum state after the qSVD is sparse, or when T is small. From the above, we see that the approximate computation of the SVD entropy using quantum devices requires $O(N_s T \log(N_s T))$ computation in a classical computing device for computing the right hand side of (9) and $O(\text{polylog}(N_s T)) \cdot \tilde{O}\left(\sqrt{\min(N_s, T)}/\epsilon^2\right)$, gate operations

in a quantum computing device. In contrast, when we exactly encode data by using $O(N_s T)$ gates (say, with the technique in [18, 41]), the total gate operations in a quantum computing device is $O(N_s T) \cdot \tilde{O}\left(\sqrt{\min(N_s, T)}/\epsilon^2\right)$, which is much larger than the one using our approximate amplitude encoding.

D. Demonstration

Here we give a numerical demonstration to show the performance of our algorithm composed of AAE and qSVD, in the problem of computing the SVD entropy for the following top four real stock data found in the Dow Jones Industrial Average at the end of 2008; Exxon Mobil Corporation (XOM), Walmart (WMT), Procter & Gamble (PG), and Microsoft (MSFT). For each stock, we use the one-year monthly data from April 2008 to March 2009. Table I shows the logarithmic rate of return (24) for each stock at every month, which was taken from Yahoo Finance (in every month, the opening price is used).

The goal is to compute the SVD entropy at each term, with the length $T = 5$ months. For example, we compute the SVD entropy at August 2008, using the data from April 2008 to August 2008. The stock indices $j = 1, 2, 3, 4$ correspond to XOM, WMT, PG, and MSFT, respectively. Also, the time indices $t = 0, 1, 2, 3, 4$ identify the month in which the SVD entropy is computed; for instance, the SVD entropy on August 2008 is computed, using the data of April 2008 ($t = 0$), May 2008 ($t = 1$), June 2008 ($t = 2$), July 2008 ($t = 3$), and August 2008 ($t = 4$). As a result, s_{jt} has totally $20 = 4$ (stocks) $\times 5$ (terms) components, and thus, from Eq. (24), both r_{jt} and a_{jt} have $16 = 4 \times 4$ components, where the indices run over $j = 1, 2, 3, 4$ and $t = 1, 2, 3, 4$; that is, $\mathcal{H}_{\text{stock}} \otimes \mathcal{H}_{\text{time}} = \mathbf{C}^4 \otimes \mathbf{C}^4$. Note that $\{a_{jt}\}$ contain both positive and negative quantities, and thus AAE algorithm for Case 2 is used for the data loading. Hence, we need an additional ancilla qubit, meaning that the total number of qubit is 5. The extended target state (7) is now given by

$$|\bar{\psi}\rangle = \sum_{k=0}^{31} \bar{\psi}_k |k\rangle, \quad (36)$$

where

$$\bar{\psi}_k = \begin{cases} a_{jt} & \text{if } k = 8(j-1) + 2(t-1), & a_{jt} \geq 0 \\ 0 & \text{if } k = 8(j-1) + 2(t-1), & a_{jt} < 0 \\ -a_{jt} & \text{if } k = 8(j-1) + 2(t-1) + 1, & a_{jt} < 0 \\ 0 & \text{if } k = 8(j-1) + 2(t-1) + 1, & a_{jt} \geq 0. \end{cases}$$

The binary representation of k corresponds to the state of the qubits, e.g., $|2\rangle \equiv |00010\rangle$. Then the conditions of perfect data loading, given by Eqs. (8) and (9), are

represented as

$$|\langle k|U(\theta)|0\rangle^{\otimes 5}|^2 = \bar{\psi}_k^2, \\ |\langle k|H^{\otimes 5}U(\theta)|0\rangle^{\otimes 5}|^2 = \left(\sum_{\ell=0}^{31} \bar{\psi}_\ell \langle \ell|H^{\otimes 5}|k\rangle\right)^2.$$

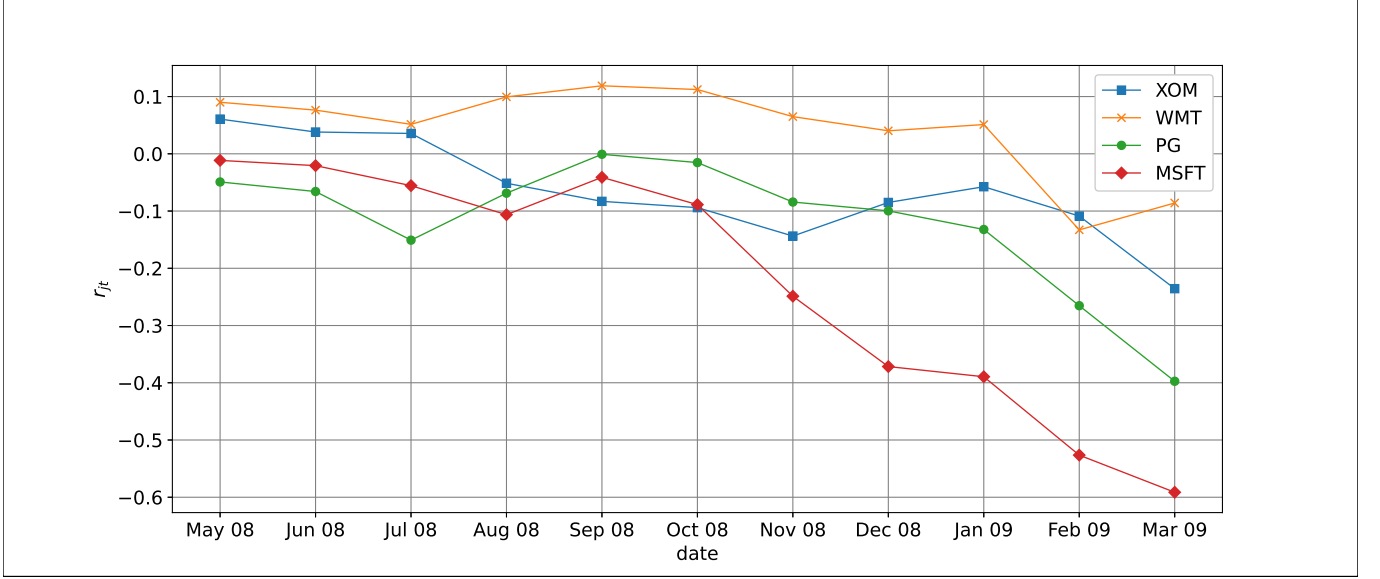
The right-hand side of these equations are the target probability distribution to be approximated by training the PQC $U(\theta)$.

In this work, we execute the AAE algorithm as follows. The PQC is the 8-layers ansatz $U(\theta)$ illustrated in Fig. 3. Each layer is composed of the set of parameterized single-qubit rotational gate $R_y(\theta_r) = \exp(-i\theta_r \sigma_y/2)$ and CNOT gates that connect adjacent qubits; θ_r is the r -th parameter and σ_y is the Pauli Y operator (hence $U(\theta)$ is a real matrix). We randomly initialize all θ_r at the beginning of each training. As the kernel function, $\kappa(x, y) = \exp(-(x-y)^2/0.25)$ is used. To compute the r -th gradient of \mathcal{L} given in Eq. (16), we generate 400 samples for each $q_{\theta_r}^+$, $q_{\theta_r}^-$, $q_{\theta_r}^{H+}$, and $q_{\theta_r}^{H-}$. As the optimizer, Adam [42] is used; the learning rate is 0.1 for the first 100 epochs and 0.01 for the other epochs. The number of iterations (i.e., the number of the updates of the parameters) is set to 300 for training $U(\theta)$. We performed 10 trials for training $U(\theta)$ and then chose the one which best minimizes the cost \mathcal{L}_{MMD} at the final iteration step.

Suppose that the above AAE algorithm generated the quantum state $|\widetilde{\text{Data}}\rangle$, which approximates Eq. (30). Then the next step is to apply the qSVD circuit to $|\widetilde{\text{Data}}\rangle$ and then compute the SVD entropy. The PQCs $U_1(\xi)$ and $U_2(\xi')$, which respectively act on the stock state $|j\rangle$ and the time state $|t\rangle$, are set to 2-qubits 8-layers ansatz illustrated in Fig 4. Each layer of U_1 is composed of parameterized single-qubit rotational gates $\exp(-i\xi_r \sigma_{a_r}/2)$ and CNOT gates that connect adjacent qubits, where ξ_r is the r -th parameter and σ_{a_r} is the Pauli operator ($a_r = x, y, z$). As seen in the figure, U_2 has almost the same structure as U_1 . Also we used Adam optimizer, with learning rate 0.01. For simulating the quantum circuit, we used Qiskit [43]. To focus on the net approximation error that stems from qSVD algorithm, we assume that the gradient of \mathcal{L}_{SVD} can be exactly computed (equivalently, infinite number of measurements are performed to compute this quantity). The number of iterations for training $U_1(\xi) \otimes U_2(\xi')|\widetilde{\text{Data}}\rangle$ is 500. Unlike the case of AAE, we performed qSVD only once, to determine the optimal parameter set $(\xi_{\text{opt}}, \xi'_{\text{opt}})$. Finally, we compute the SVD entropy based on the amplitude of the final state $U_1(\xi_{\text{opt}}) \otimes U_2(\xi'_{\text{opt}})|\widetilde{\text{Data}}\rangle$, under the assumption that the ideal quantum state tomography can be executed.

The SVD entropies in each term, computed through AAE and qSVD algorithms, is shown by the orange line with square dots in Fig. 5. As a reference, the exact value of SVD entropy, computed by diagonalizing the correlation matrix, is shown by the blue line with circle dots. Also, to see a distinguishing property of

Symbol	Apr 08	May 08	Jun 08	Jul 08	Aug 08	Sep 08	Oct 08	Nov 08	Dec 08	Jan 09	Feb 09	Mar 09
XOM	84.80	90.10	88.09	87.87	80.55	78.04	77.19	73.45	77.89	80.06	76.06	67.00
WMT	53.19	58.20	57.41	56.00	58.75	59.90	59.51	56.76	55.37	55.98	46.57	48.81
PG	70.41	67.03	65.92	60.55	65.73	70.35	69.34	64.72	63.73	61.69	54.00	47.32
MSFT	28.83	28.50	28.24	27.27	25.92	27.67	26.38	22.48	19.88	19.53	17.03	15.96

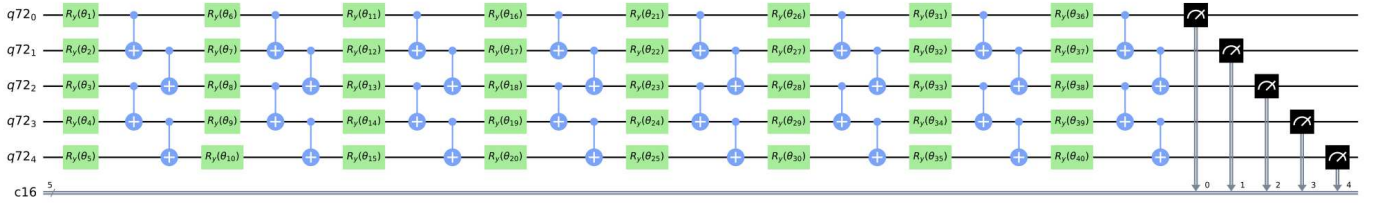
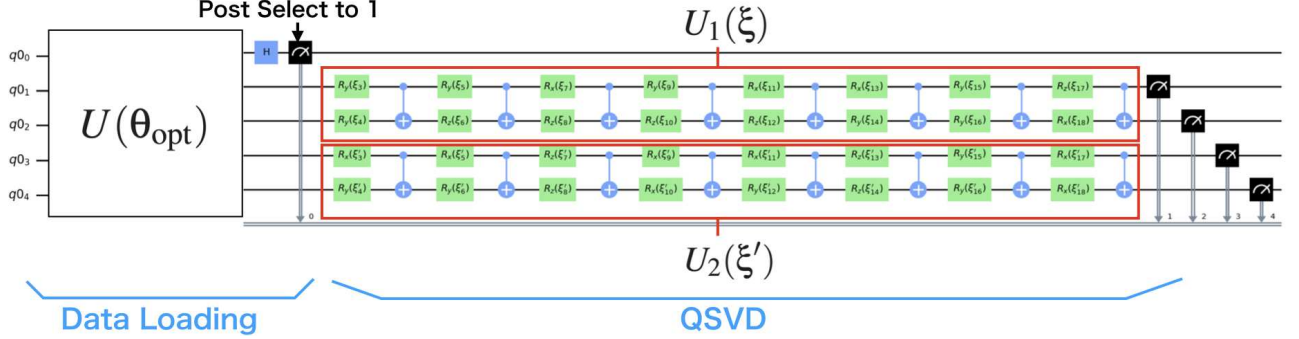
TABLE I: Logarithmic rate of return r_{jt} defined by Eq. (24).FIG. 2: Logarithmic rate of return (r_{jt}) for each stock and each moment that is computed with the data in Table I.

AAE, we study the naive data-loading algorithm that trains the PQC $U_{\text{naive}}(\theta)$ so that it learns only the absolute value of the data by minimizing the cost function $\mathcal{L}_{\text{MMD}}(|\langle j|t|U_{\text{naive}}(\theta)|0\rangle^{\otimes 4}|^2, a_{jt}^2)$; namely, $U_{\text{naive}}(\theta)$ loads the data so that the absolute values of the amplitudes of $U_{\text{naive}}(\theta)|0\rangle^{\otimes 4}$ is close to $|a_{jt}|$ yet without taking into account the signs. The resulting value of SVD entropy computed with this naive method is shown by the green line with cross marks. Importantly, the SVD entropies computed with our AAE algorithm well approximate the exact values, while the naive method poorly works at some point of term. Note that the estimation errors in the case of AAE is within the acceptable range for application, because the SVD entropy usually fluctuates by several percent during the normal period, while it can change drastically by a few tens of percent at around financial events [22, 44–46].

In Fig. 6, as examples, we show the training results of $q_\theta(k) = |\langle k|U(\theta)|0\rangle^{\otimes 5}|^2$ and $q_\theta^H(k) = |\langle k|H^{\otimes 5}U(\theta)|0\rangle^{\otimes 5}|^2$ for four terms Apr 08-Aug 08, May 08-Sep 08, Jun 08-Oct 08, and Jul 08-Nov 08 (green lines); these are the best one out of 10 trials, which minimizes the cost $\mathcal{L}_{\text{MMD}}(\theta)$ at the 200-th iteration step. Also the corresponding target distributions $p(k) = \bar{\psi}_k^2$ and $p^H(k) = \left(\sum_{\ell=0}^{31} \bar{\psi}_\ell \langle \ell|H^{\otimes 5}|k\rangle\right)^2$ are illustrated with green bars.

The right column of Fig. 6 plots the change of the costs $\mathcal{L}_{\text{MMD}}(q_\theta, p)$, $\mathcal{L}_{\text{MMD}}(q_\theta^H, p^H)$, and $\mathcal{L}_{\text{MMD}}(\theta) = (\mathcal{L}_{\text{MMD}}(q_\theta, p) + \mathcal{L}_{\text{MMD}}(q_\theta^H, p^H))/2$ for each term. These results confirm that the AAE algorithm realizes almost perfect data-loading; that is, the model distributions q_θ and q_θ^H converge to the target distributions p and p^H , respectively, which eventually leads to the successful computation of SVD entropy.

Lastly, we point out the interesting feature of the SVD entropy, which can be observed from Figs. 2 and 5. Figure 2 shows that, until August 2008, the stocks did not strongly correlate with each other, which leads to the relatively large value of SVD entropy (~ 0.9) as seen in Fig. 5. On September 2008, the Lehman Brothers bankruptcy ignited the global financial crisis. As a result, from October 2008 to February 2009, the stocks became strongly correlated with each other. In such a case, many of stocks cooperatively declined as seen in Fig. 2. This strong correlation led to the small SVD entropy (~ 0.7) from October to February, which is an evidence of the financial crisis. On March 2009, Fig. 5 shows that the SVD entropy again takes relatively large value (~ 0.9), indicating that the market returned to normal and each stock moved differently. Interestingly, according to the S&P index, it is argued that the financial crisis ended on March 2009 (e.g., see [47]), which is consistent

FIG. 3: The structure of $U(\theta)$.FIG. 4: The structure of the circuit that performs qSVD. The parameters θ_{opt} in the data loading circuit are fixed.

to the result of SVD entropy. We would like to emphasize that AAE algorithm correctly computed the SVD entropy and enables us to capture the above-mentioned financial trends.

IV. CONCLUSIONS

This paper provides the Approximate Amplitude Encoding (AAE) algorithm that effectively loads a given classical data into a shallow parameterized quantum circuit. The point of the AAE algorithm is in the formulation of a valid cost function composed of two types of maximum mean discrepancy measures, based on the perfect encoding condition (Theorem 1 for Case 1 and Theorem 2 for Case 2); training of the circuit is executed by minimizing this cost function, which enables encoding the signs of the data components unlike the previous proposal. We also provide an algorithm composed of AAE

and the existing quantum singular value decomposition (qSVD) algorithm, for computing the SVD entropy in the stock market. A thorough numerical study was performed, showing that the approximation error of AAE was found to be sufficiently small in this case and, as a result, the subsequent qSVD algorithm yields a good approximation solution. We believe that the proposed AAE algorithm paves the way to implement various quantum algorithms that process classical data such as HHL, by reducing the highly demanding resources of quantum devices.

Acknowledgments

This work was supported by MEXT Quantum Leap Flagship Program Grant Number JPMXS0118067285 and JPMXS0120319794.

-
- [1] P. Shor. Algorithms for quantum computation: discrete logarithms and factoring. Proceedings 35th Annual Symposium on Foundations of Computer Science, pages 124–134, 1994.
- [2] L. K. Grover. A fast quantum mechanical algorithm for database search. In STOC '96, 1996.

- [3] A. W. Harrow, A. Hassidim and S. Lloyd. Quantum algorithm for linear systems of equations. Physical review letters, 103(15):150502, 2009.
- [4] J. Biamonte *et al.* Quantum machine learning. Nature, 549(7671):195–202, 2017.
- [5] S. Srinivasan, C. Downey and B. Boots. Learning and in-

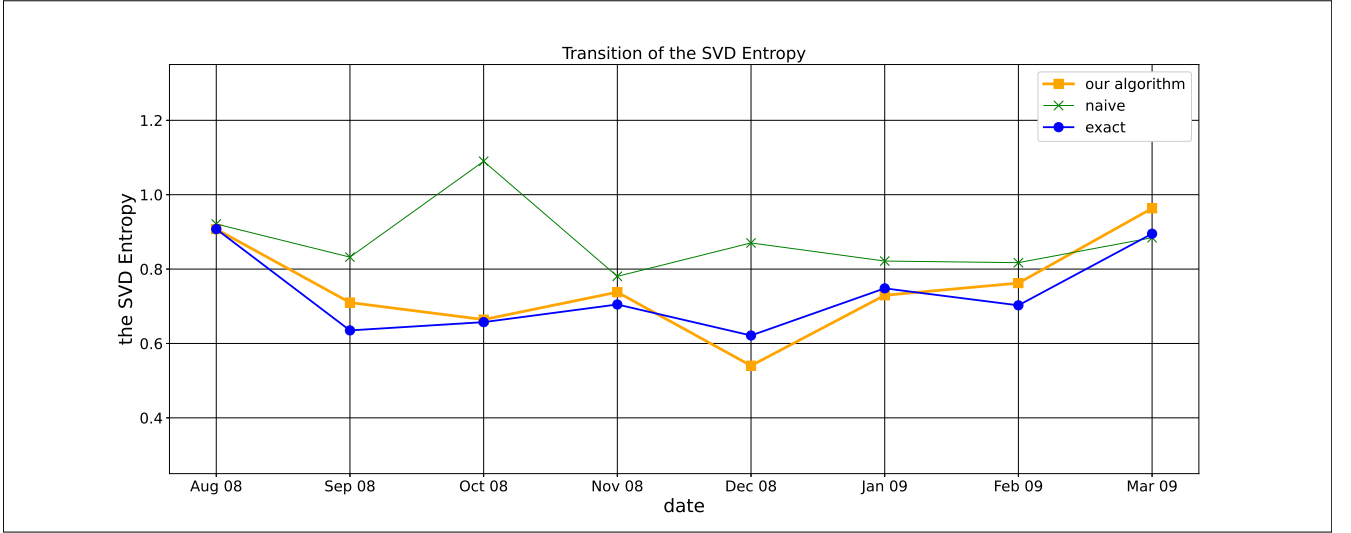


FIG. 5: Change of the SVD entropy for each term.

- ference in hilbert space with quantum graphical models. In *Advances in Neural Information Processing Systems*, pages 10338–10347, 2018.
- [6] M. Schuld, I. Sinayskiy and F. Petruccione. Prediction by linear regression on a quantum computer. *Physical Review A*, 94(2):022342, 2016.
- [7] V. Havlíček *et al.* Supervised learning with quantum-enhanced feature spaces. *Nature*, 567(7747):209–212, 2019.
- [8] C. Ciliberto *et al.* Quantum machine learning: a classical perspective. *Proceedings of the Royal Society A: Mathematical, Physical and Engineering Sciences*, 474(2209):20170551, 2018.
- [9] M. Schuld *et al.* Circuit-centric quantum classifiers. *Physical Review A*, 101(3):032308, 2020.
- [10] C. Blank *et al.* Quantum classifier with tailored quantum kernel. *npj Quantum Information*, 6(1):1–7, 2020.
- [11] M. Schuld *et al.* Circuit-centric quantum classifiers. *Physical Review A*, 101(3):032308, 2020.
- [12] P. Rebentrost, M. Mohseni and S. Lloyd. Quantum support vector machine for big data classification. *Physical review letters*, 113(13):130503, 2014.
- [13] I. Kerenidis and A. Prakash. Quantum recommendation systems. *arXiv preprint arXiv:1603.08675*, 2016.
- [14] N. Wiebe, D. Braun and S. Lloyd. Quantum algorithm for data fitting. *Physical review letters*, 109(5):050505, 2012.
- [15] M. Schuld, M. Fingerhuth and F. Petruccione. Implementing a distance-based classifier with a quantum interference circuit. *EPL (Europhysics Letters)*, 119(6):60002, 2017.
- [16] L. K. Grover. Synthesis of quantum superpositions by quantum computation. *Physical review letters*, 85(6):1334, 2000.
- [17] Y. R. Sanders *et al.* Black-box quantum state preparation without arithmetic. *Physical review letters*, 122(2):020502, 2019.
- [18] M. Plesch and Č. Brukner. Quantum-state preparation with universal gate decompositions. *Physical Review A*, 83(3):032302, 2011.
- [19] V. V. Shende, S. S. Bullock and I. L. Markov. Synthesis of quantum-logic circuits. *IEEE Transactions on Computer-Aided Design of Integrated Circuits and Systems*, 25(6):1000–1010, 2006.
- [20] C. Zoufal, A. Lucchi and S. Woerner. Quantum generative adversarial networks for learning and loading random distributions. *npj Quantum Information*, 5(1):1–9, 2019.
- [21] C. Bravo-Prieto, D. García-Martín and J. I. Latorre. Quantum singular value decomposer. *Physical Review A*, 101(6):062310, 2020.
- [22] P. Caraianni. The predictive power of singular value decomposition entropy for stock market dynamics. *Physica A: Statistical Mechanics and its Applications*, 393:571–578, 2014.
- [23] N. Ahmed and K. R. Rao. Walsh-hadamard transform. In *Orthogonal Transforms for Digital Signal Processing*, pages 99–152. Springer, 1975.
- [24] J.-G. Liu and L. Wang. Differentiable learning of quantum circuit born machines. *Physical Review A*, 98(6):062324, 2018.
- [25] B. Coyle *et al.* The born supremacy: Quantum advantage and training of an ising born machine. *npj Quantum Information*, 6(1):1–11, 2020.
- [26] B. K. Sriperumbudur *et al.* Injective hilbert space embeddings of probability measures. In *COLT*, 2008.
- [27] K. Fukumizu *et al.* Kernel measures of conditional dependence. In *NIPS*, 2007.
- [28] B. K. Sriperumbudur *et al.* On integral probability metrics, ϕ -divergences and binary classification. *arXiv: Information Theory*, 2009.
- [29] A. Harrow and J. Napp. Low-depth gradient measurements can improve convergence in variational hybrid quantum-classical algorithms. *arXiv: Quantum Physics*, 2019.
- [30] G. Brassard *et al.* Quantum amplitude amplification and estimation. *Contemporary Mathematics*, 305:53–74, 2002.
- [31] S. Aaronson and P. Rall. Quantum approximate counting, simplified. *ArXiv*, abs/1908.10846, 2020.
- [32] K. Nakaji. Faster amplitude estimation. *Quantum Inf.*

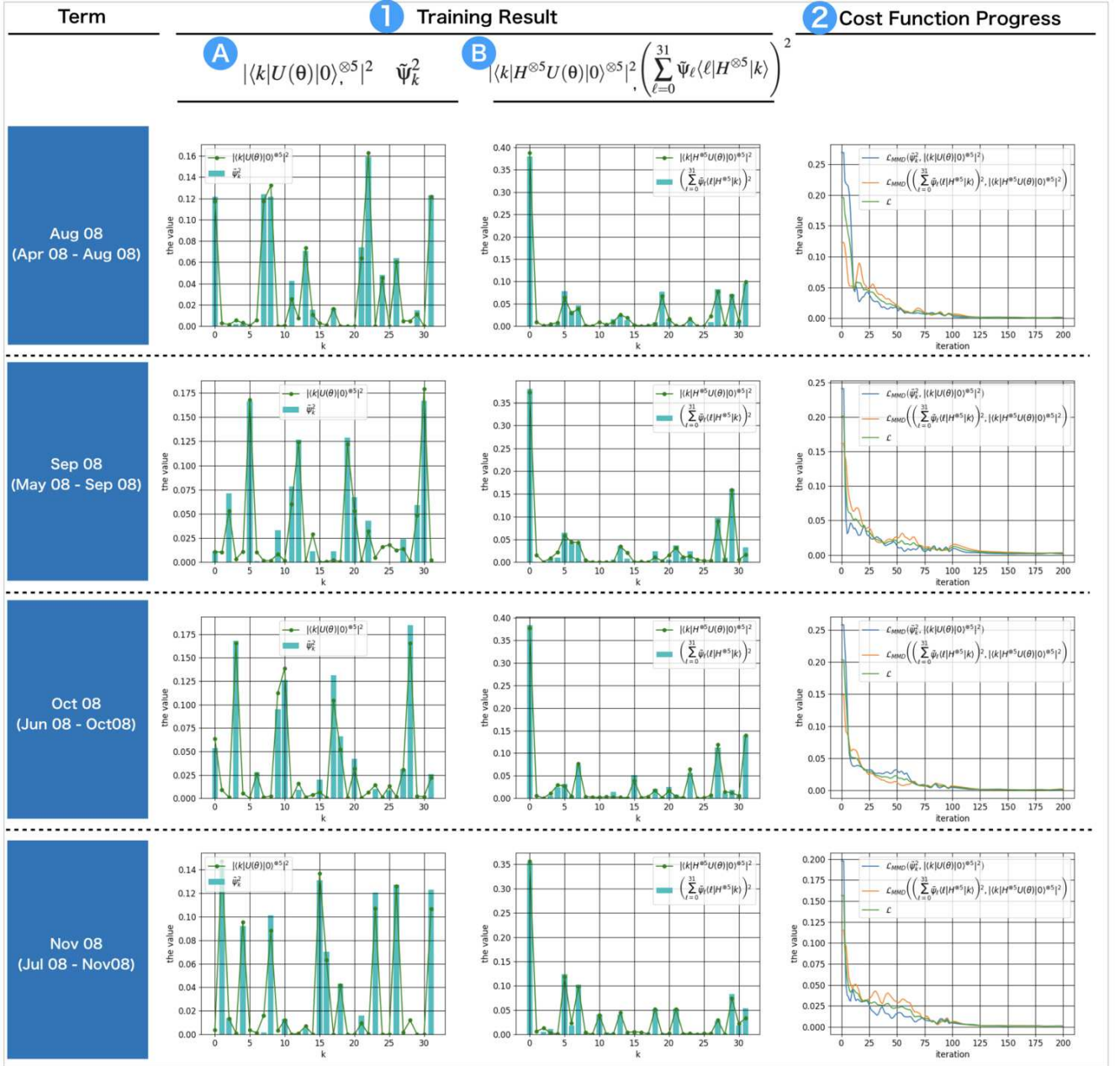


FIG. 6: ①: The training results of $|\langle k|U(\theta)|0\rangle|^{\otimes 5}|^2$ and $|\langle k|H^{\otimes 5}U(\theta)|0\rangle|^{\otimes 5}|^2$ for each term (green lines) and the corresponding target distributions: $\tilde{\Psi}_k^2$ and $\left(\sum_{\ell=0}^{31} \tilde{\Psi}_{\ell}\langle \ell|H^{\otimes 5}|k\rangle\right)^2$ (green bars). The training results for each term are the ones when the cost function \mathcal{L} at the 200-th epoch becomes the smallest in 10 trials. ②: The progress of the cost function \mathcal{L} in the same trial as ① for each term. In the same figures, we also show the progress of the cost functions for two distributions: $|\langle k|U(\theta)|0\rangle|^{\otimes 5}|^2$ and $|\langle k|H^{\otimes 5}U(\theta)|0\rangle|^{\otimes 5}|^2$, that contribute to \mathcal{L} .

Comput., 20:1109–1122, 2020.

- [33] I. Goodfellow *et al.* Generative adversarial nets. In Z. Ghahramani *et al.*, editors, *Advances in Neural Information Processing Systems 27*, pages 2672–2680. Curran Associates, Inc., 2014.
- [34] L. Laloux *et al.* Noise dressing of financial correlation matrices. *Physical review letters*, 83(7):1467, 1999.
- [35] V. Plerou *et al.* Universal and nonuniversal properties of cross correlations in financial time series. *Physical review*

letters, 83(7):1471, 1999.

- [36] V. Plerou *et al.* Random matrix approach to cross correlations in financial data. *Physical Review E*, 65(6):066126, 2002.
- [37] A. Utsugi, K. Ino and M. Oshikawa. Random matrix theory analysis of cross correlations in financial markets. *Physical Review E*, 70(2):026110, 2004.
- [38] A. Dutta *et al.* Quantum phase transitions in transverse field spin models: from statistical physics to quantum

information. Cambridge University Press, 2015.

- [39] H. Matsueda. Renormalization group and curved space-time. arXiv preprint arXiv:1106.5624, 2011.
- [40] T. Li and X. Wu. Quantum query complexity of entropy estimation. IEEE Transactions on Information Theory, 65(5):2899–2921, 2018.
- [41] V. Bergholm *et al.* Quantum circuits with uniformly controlled one-qubit gates. Physical Review A, 71(5), 2005.
- [42] D. P. Kingma and J. Ba. Adam: A method for stochastic optimization. arXiv preprint arXiv:1412.6980, 2014.
- [43] H. Abraham *et al.* Qiskit: An open-source framework for quantum computing, 2019.
- [44] R. Gu, W. Xiong and X. Li. Does the singular value decomposition entropy have predictive power for stock market? evidence from the shenzhen stock market. Physica A: Statistical Mechanics and its Applications, 439:103–113, 2015.
- [45] J. Civitarese. Volatility and correlation-based systemic risk measures in the us market. Physica A: Statistical Mechanics and its Applications, 459:55–67, 2016.
- [46] P. Caraianni. Modeling the comovement of entropy between financial markets. Entropy, 20(6):417, 2018.
- [47] K. Manda, F. Advisor and M. Brenner. Stock market volatility during the 2008 financial crisis, 2010.

Appendix A: Proof of the Theorem 1

Theorem 1. *In Case 1, if (4) and (5) are exactly satisfied, $U(\theta)|0\rangle = \sum_j \mathbf{d}_j|j\rangle$ or $U(\theta)|0\rangle = -\sum_j \mathbf{d}_j|j\rangle$.*

Proof. Let us denote \mathbf{a}_j by $\langle j|U(\theta)|0\rangle$. Then, (4) and (5) are rewritten as

$$\mathbf{a}_j^2 = \mathbf{d}_j^2 \quad (\forall j) \quad (\text{A1})$$

$$\left(\sum_{k=0}^{N-1} H_{jk}^{\otimes n} \mathbf{a}_k \right)^2 = \left(\sum_{k=0}^{N-1} H_{jk}^{\otimes n} \mathbf{d}_k \right)^2 \quad (\forall j) \quad (\text{A2})$$

where $H_{jk}^{\otimes n} \equiv \langle j|H^{\otimes n}|k\rangle$. For $j = 0$, the left hand side of (A2) becomes

$$\left(\sum_{k=0}^{N-1} H_{0k}^{\otimes n} \mathbf{a}_k \right)^2 = \frac{1}{2^n} \left(\sum_{k=0}^{N-1} \mathbf{a}_k \right)^2 \leq \frac{1}{2^n} \left(\sum_{k=0}^{N-1} |\mathbf{a}_k| \right)^2 \quad (\text{A3})$$

where the equality holds only when $\mathbf{a}_k \geq 0$ ($\forall k$) or $\mathbf{a}_k \leq 0$ ($\forall k$). The equality condition is equivalent to $\mathbf{a} = \mathbf{d}$ or $\mathbf{a} = -\mathbf{d}$, because of (A1) and the condition of Case 1: $\mathbf{d}_j \geq 0$ ($\forall j$) or $\mathbf{d}_j \leq 0$ ($\forall j$). Conversely, if the equality condition is not satisfied, we find that

$$\begin{aligned} \frac{1}{2^n} \left(\sum_{k=0}^{N-1} \mathbf{a}_k \right)^2 &< \frac{1}{2^n} \left(\sum_{k=0}^{N-1} |\mathbf{a}_k| \right)^2 = \frac{1}{2^n} \left(\sum_{k=0}^{N-1} \mathbf{d}_k \right)^2 \\ &= \left(\sum_{k=0}^{N-1} H_{0k}^{\otimes n} \mathbf{d}_k \right)^2, \end{aligned} \quad (\text{A4})$$

which contradicts to (A2) for $j = 0$. Thus, the equality condition of (A3) is satisfied, i.e., $\mathbf{a} = \mathbf{d}$ or $\mathbf{a} = -\mathbf{d}$. \square

Appendix B: Studies regarding the improvement of our algorithm

In our algorithm we train the data loading circuit by using the measurement results in the computational basis and the Hadamard basis. However, it is possible to use the other basis; namely, given X as an orthogonal operator, we can train $U(\theta)$ so that

$$|\langle j|U(\theta)|0\rangle^{\otimes n}|^2 = \mathbf{d}_j^2 \quad (\text{B1})$$

$$|\langle j|XU(\theta)|0\rangle^{\otimes n}|^2 = \left(\sum_{k=0}^{N-1} \mathbf{d}_k \langle j|X|k\rangle \right)^2. \quad (\text{B2})$$

Then, the question is whether there exists X such that $U(\theta)|0\rangle = \sum_j \mathbf{d}_j|j\rangle$ or $U(\theta)|0\rangle = -\sum_j \mathbf{d}_j|j\rangle$ is satisfied when (B1) and (B2) hold. In the following, we show that there exists such X but it is difficult to find it for arbitrary \mathbf{d} .

As the preparation, we define the $n \times n$ row switching matrix $A^{(n)}[j, k]$ as

$$A^{(n)}[j, k] = \begin{pmatrix} 1 & & & & & \\ & \ddots & & & & \\ & & 1 & & & \\ & & 0 & & 1 & \\ & & & 1 & & \\ & & & & \ddots & \\ & & & & & 1 & 0 \\ & & 1 & & & & & 1 \\ & & & & & & & \ddots \\ & & & & & & & & 1 \end{pmatrix} \quad (0 \leq j \neq k \leq n-1) \quad (\text{B3})$$

that can be created by swapping the row j and the row k of the identity matrix. Then, given a $n \times n$ matrix R , the matrix product $A^{(n)}[j, k]R$ is the matrix produced by exchanging the row j and the row k of R and the matrix product $RA^{(n)}[j, k]$ is the matrix produced by exchanging the column j and the column k of R . We denote by $\mathcal{A}(n)$ as the set of the $n \times n$ matrices that can be written as the product of $A^{(n)}[j, k]$ s (for example $A^{(8)}[0, 2]A^{(8)}[4, 7]A^{(8)}[2, 3] \in \mathcal{A}(8)$). By using the above notations, we give the following definition for the pair of a vector and a square matrix.

Definition 1. Let \mathbf{k} be a column vector, $\dim(\mathbf{k})$ be the number of columns of \mathbf{k} , and A be a square matrix that has $\dim(\mathbf{k})$ columns/rows. The pair (\mathbf{k}, A) is said to be **pair-block-diagonal** if there exists $P, Q \in \mathcal{A}(\dim(\mathbf{k}))$ that transforms \mathbf{k} and A as $\mathbf{k}' = Q\mathbf{k}$ and $A' = PAQ$ where \mathbf{k}' and A' are splittable as

$$\mathbf{k}' = \begin{pmatrix} \mathbf{k}_\uparrow \\ \mathbf{k}_\downarrow \end{pmatrix}, \quad A' = \begin{pmatrix} A_{\uparrow\uparrow} & A_{\uparrow\downarrow} \\ A_{\downarrow\uparrow} & A_{\downarrow\downarrow} \end{pmatrix} \quad (\text{B4})$$

so that $A_{\uparrow\downarrow}\mathbf{k}_\downarrow = 0, A_{\downarrow\uparrow}\mathbf{k}_\uparrow = 0$. Here $\mathbf{k}_\uparrow, \mathbf{k}_\downarrow \neq 0$ and the number of rows in $A_{\uparrow\uparrow}$ and $A_{\uparrow\downarrow}$ is the same as that of

\mathbf{k}_\uparrow . The P is said to be a **left-pair-block-generator** and the Q is said to be a **right-pair-block-generator**.

By using the definition, we can state the following theorem:

Theorem 3. Suppose that X is an $N \times N$ real matrix. There exist N -element real vectors $\mathbf{d}' (\neq \mathbf{d}, -\mathbf{d})$ and $\mathbf{c}' = X\mathbf{d}'$ that satisfy

$$\mathbf{d}'^2 = \mathbf{d}_j^2, \mathbf{c}'^2 = \mathbf{c}_j^2 \quad (\forall j \in [0, 1, \dots, N-1]) \quad (\text{B5})$$

if and only if the combination (\mathbf{d}, X) is pair-block-diagonal where \mathbf{c} is an N -element vector that satisfies

$$\mathbf{c} = X\mathbf{d}. \quad (\text{B6})$$

Proof. Firstly we prove the sufficient condition of the theorem. If the sufficient assumption is satisfied, there exist a left-pair-block-generator P and a right-pair-block-generator Q . By using $Q^2 = I$, (B6) can be transformed into

$$P\mathbf{c} = (PXQ)(Q\mathbf{d}). \quad (\text{B7})$$

From the definition of pair-block-diagonal, PXQ and $Q\mathbf{d}$ are block composed

$$PXQ = \begin{pmatrix} X_{\uparrow\uparrow} & X_{\uparrow\downarrow} \\ X_{\downarrow\uparrow} & X_{\downarrow\downarrow} \end{pmatrix}, \quad Q\mathbf{d} = \begin{pmatrix} \mathbf{d}_\uparrow \\ \mathbf{d}_\downarrow \end{pmatrix} \quad (\text{B8})$$

where the number of columns of $X_{\uparrow\uparrow}$ and $X_{\uparrow\downarrow}$ equals to the number of rows of \mathbf{d}_\uparrow , and

$$X_{\uparrow\downarrow}\mathbf{d}_\downarrow = 0, \quad X_{\downarrow\uparrow}\mathbf{d}_\uparrow = 0. \quad (\text{B9})$$

Note that $\mathbf{d}_\uparrow, \mathbf{d}_\downarrow \neq 0$ and

$$\mathbf{d} = Q \begin{pmatrix} \mathbf{d}_\uparrow \\ \mathbf{d}_\downarrow \end{pmatrix}. \quad (\text{B10})$$

Substituting (B8) and (B9) into (B7), we get

$$P\mathbf{c} = \begin{pmatrix} X_{\uparrow\uparrow}\mathbf{d}_\uparrow \\ X_{\downarrow\downarrow}\mathbf{d}_\downarrow \end{pmatrix}, \quad (\text{B11})$$

and therefore,

$$\mathbf{c} = P \begin{pmatrix} X_{\uparrow\uparrow}\mathbf{d}_\uparrow \\ X_{\downarrow\downarrow}\mathbf{d}_\downarrow \end{pmatrix} \quad (\text{B12})$$

holds because $P^2 = I$. If we set

$$\mathbf{d}' = Q \begin{pmatrix} \mathbf{d}_\uparrow \\ -\mathbf{d}_\downarrow \end{pmatrix} \quad (\text{B13})$$

then

$$\mathbf{c}' = X\mathbf{d}' = P(PXQ) \begin{pmatrix} \mathbf{d}_\uparrow \\ -\mathbf{d}_\downarrow \end{pmatrix} = P \begin{pmatrix} X_{\uparrow\uparrow}\mathbf{d}_\uparrow \\ -X_{\downarrow\downarrow}\mathbf{d}_\downarrow \end{pmatrix}. \quad (\text{B14})$$

Because P, Q are matrices that interchange rows, comparing (B13) and (B10); (B14) and (B12), we see that

$$\mathbf{d}'^2 = \mathbf{d}_j^2, \quad \mathbf{c}'^2 = \mathbf{c}_j^2, \quad \mathbf{d}' \neq \mathbf{d}, -\mathbf{d} \quad (\text{B15})$$

which concludes the proof of the sufficient condition of the theorem.

Next, we prove the necessity condition of the theorem. If the necessity assumption holds, there exist \mathbf{d}' and \mathbf{c}' that satisfy $\mathbf{c}' = X\mathbf{d}'$ and (B5). We set

$$\mathbf{c}^+ = \frac{\mathbf{c} + \mathbf{c}'}{2}, \mathbf{c}^- = \frac{\mathbf{c} - \mathbf{c}'}{2}. \quad (\text{B16})$$

Then for each element of $\mathbf{c}^-, \mathbf{c}^+$, it holds that

$$\mathbf{c}_j^+ = \begin{cases} \mathbf{c}_j & (\text{if } \mathbf{c}_j = \mathbf{c}'_j) \\ 0 & (\text{if } \mathbf{c}_j = -\mathbf{c}'_j) \end{cases} \\ \mathbf{c}_j^- = \begin{cases} 0 & (\text{if } \mathbf{c}_j = \mathbf{c}'_j) \\ \mathbf{c}_j & (\text{if } \mathbf{c}_j = -\mathbf{c}'_j) \end{cases}. \quad (\text{B17})$$

We see that \mathbf{c}_j^- is non-zero only if \mathbf{c}_j^+ is zero, and vice versa. Therefore, by using a row swap matrix $P \in \mathcal{A}(N)$, \mathbf{c}_i^- and \mathbf{c}_i^+ can be transformed as

$$P\mathbf{c}^+ = \begin{pmatrix} \mathbf{c}^\uparrow \\ \mathbf{0} \end{pmatrix}, P\mathbf{c}^- = \begin{pmatrix} \mathbf{0} \\ \mathbf{c}^\downarrow \end{pmatrix} \quad (\text{B18})$$

where $\dim(\mathbf{c}^\uparrow) + \dim(\mathbf{c}^\downarrow) = N$. Similarly, we set

$$\mathbf{d}^+ = \frac{\mathbf{d} + \mathbf{d}'}{2}, \mathbf{d}^- = \frac{\mathbf{d} - \mathbf{d}'}{2}. \quad (\text{B19})$$

Then \mathbf{d}_j^- is non-zero only if \mathbf{d}_j^+ is zero, and vice versa. Thus, by using another row swap matrix $Q \in \mathcal{A}(N)$,

$$Q\mathbf{d}^+ = \begin{pmatrix} \mathbf{d}^\uparrow \\ \mathbf{0} \end{pmatrix}, Q\mathbf{d}^- = \begin{pmatrix} \mathbf{0} \\ \mathbf{d}^\downarrow \end{pmatrix} \quad (\text{B20})$$

where $\dim(\mathbf{d}^\uparrow) + \dim(\mathbf{d}^\downarrow) = N$. From $\mathbf{c}' = X\mathbf{d}'$ and (B6),

$$\mathbf{c}^+ = X\mathbf{d}^+. \quad (\text{B21})$$

By multiplying P from left and using $Q^2 = I$, we get

$$P\mathbf{c}^+ = PXQQ\mathbf{d}^+. \quad (\text{B22})$$

Substituting the first equality in (B18) and that in (B20) into (B22),

$$\begin{pmatrix} \mathbf{c}^\uparrow \\ \mathbf{0} \end{pmatrix} = \begin{pmatrix} X_{\uparrow\uparrow} & X_{\uparrow\downarrow} \\ X_{\downarrow\uparrow} & X_{\downarrow\downarrow} \end{pmatrix} \begin{pmatrix} \mathbf{d}^\uparrow \\ \mathbf{0} \end{pmatrix} \quad (\text{B23})$$

where we split PXQ into submatrices so that the number of rows and columns of $X_{\uparrow\uparrow}$ is $\dim(\mathbf{d}^\uparrow)$ and $\dim(\mathbf{c}^\uparrow)$

respectively. Writing the equality in (B23) explicitly, we get

$$\mathbf{c}_\uparrow = X_{\uparrow\uparrow}\mathbf{d}_\uparrow, \quad (\text{B24})$$

$$\mathbf{0} = X_{\downarrow\uparrow}\mathbf{d}_\uparrow. \quad (\text{B25})$$

Similarly, we obtain

$$\begin{pmatrix} \mathbf{0} \\ \mathbf{c}_\downarrow \end{pmatrix} = \begin{pmatrix} X_{\uparrow\uparrow} & X_{\uparrow\downarrow} \\ X_{\downarrow\uparrow} & X_{\downarrow\downarrow} \end{pmatrix} \begin{pmatrix} \mathbf{0} \\ \mathbf{d}_\downarrow \end{pmatrix} \quad (\text{B26})$$

and as a result,

$$\mathbf{0} = X_{\uparrow\downarrow}\mathbf{d}_\downarrow, \quad (\text{B27})$$

$$\mathbf{c}_\downarrow = X_{\downarrow\downarrow}\mathbf{d}_\downarrow. \quad (\text{B28})$$

Since

$$\begin{pmatrix} \mathbf{d}_\uparrow \\ \mathbf{d}_\downarrow \end{pmatrix} = Q\mathbf{d}, \quad PXQ = \begin{pmatrix} X_{\uparrow\uparrow} & X_{\uparrow\downarrow} \\ X_{\downarrow\uparrow} & X_{\downarrow\downarrow} \end{pmatrix}, \quad (\text{B29})$$

the equations (B25) and (B27) indicate that (\mathbf{d}, X) is pair-block-diagonal. \square

From the theorem, it seems that when a dataset (hence \mathbf{d}) is given, we should find X that (\mathbf{d}, X) is *not* pair-block-diagonal; then by training $U(\theta)$ so that (B1) and (B2) with the X , the goal (3) is achieved. However, as far as our knowledge, for general \mathbf{d} , it is difficult to check if (\mathbf{d}, X) is pair-block-diagonal or not. On the other hand, if $\mathbf{d}_j \geq 0$ ($\forall j$) or $\mathbf{d}_j \leq 0$ ($\forall j$), we can show that $(\mathbf{d}, H^{\otimes n})$ is *not* pair-block-diagonal; although we already know the fact from the Theorem 1, we can also prove it by directly showing that the condition for pair-block-diagonal is not satisfied when $\mathbf{d}_j \geq 0$ ($\forall j$) or $\mathbf{d}_j \leq 0$ ($\forall j$) and $X = H^{\otimes n}$. Therefore, instead of finding X for general \mathbf{d} , we build our algorithm depending on the values of \mathbf{d} .